The C-terminal region as a modulator of rNa$_v$1.7 and rNa$_v$1.8 expression levels

Kausalia Vijayaragavan, Said Acharfi, Mohamed Chahine*

Laval University, Department of Medicine, and Laval Hospital, Research Centre, 2725 chemin Sainte-Foy, Sainte-Foy, QC, Canada G1V 4G5

Received 10 December 2003; revised 31 December 2003; accepted 5 January 2004

First published online 15 January 2004

Edited by Maurice Montal

Abstract Mammalian cells poorly express rNa$_v$1.8 channels. In contrast, rNa$_v$1.7 dorsal root ganglion channels have 90-fold higher peak Na$^+$ current densities. We investigated the role of rNa$_v$1.7 and rNa$_v$1.8 carboxy-termini in modulating the expression of rNa$_v$1.7 and rNa$_v$1.8 channels in tsA201 cells. Mutations in the ubiquitination site of the C-terminus did not improve rNa$_v$1.8 current levels. However, rNa$_v$1.8 chimeras containing the entire or the proximal portion of the rNa$_v$1.7 C-terminus expressed 3.2-fold and 4.8-fold higher peak current densities, respectively, than parent rNa$_v$1.8 channels. We conclude that the two Na$^+$ channels may have different endoplasmic reticulum processing signals.

Key words: Voltage-gated Na$^+$ channel; C-terminus; rNa$_v$1.7; rNa$_v$1.8; tsA201; Dorsal root ganglion

1. Introduction

Voltage-gated Na$^+$ channels play an important role in the initiation and generation of action potentials in excitable cells. Ten different Na$^+$ channel isoforms have been identified by molecular cloning and at least six of them are expressed in the nervous system [1]. Tetrodotoxin-sensitive (TTX-S) Na$_v$1.7 and tetrodotoxin-resistant (TTX-R) Na$_v$1.8 are two isoforms that are predominantly expressed in the large/medium and small diameter sensory neurons of the dorsal root ganglion, respectively [2–4].

We previously described the heterologous expression of cloned rat Na$_v$1.7 (rNa$_v$1.7) and Na$_v$1.8 (rNa$_v$1.8) channels in *Xenopus* oocytes [5]. We showed that the current expression of rNa$_v$1.7 is five- to six-fold higher than that of rNa$_v$1.8 and that co-expression of the auxiliary β subunit (β_1 subunit) up-regulates the expression of Na$_v$1.8 in *Xenopus* oocytes [5]. Unlike rNa$_v$1.7, which expresses nanoampere levels of current, small or no functional expression is observable after transient transfection of rNa$_v$1.8 cDNA into tsA201 cells (human embryonic kidney HEK293-derived cell line). Interestingly, several *trans*-acting factors such as the annexin II light chain (p11) [6,7], SNS-associated protein-1 [8] and the β_3 subunit are reported to modulate the trafficking and increase the functional expression of Na$_v$1.8 in heterologous cells [9]. However, none of these factors up-regulates the expression of rNa$_v$1.8 channels in heterologous cells to levels similar to that found in C-fibers or even to levels similar to that of rNa$_v$1.7 in tsA201 cells. This suggests that either rNa$_v$1.7 possesses a forward trafficking signal, which is absent in rNa$_v$1.8, and which allows the expression of rNa$_v$1.7 channels in these mammalian cell lines, or that rNa$_v$1.8 possesses an inhibitory or retention sequence that prevents the export of the channels to the plasma membrane. The cytoplasmic carboxy-termini of cardiac voltage-gated Na$^+$ channels (Na$_v$1.5) and epithelial Na$^+$ channels (ENaC) possess a ubiquitin-protein ligase binding site (PY motif: PPxY consensus, where x is any amino acid) that promotes internalization and degradation of the channels [10,11]. Furthermore, the C-terminal segment of K$^+$ channels expresses a strong endoplasmic reticulum (ER) export signal [12,13].

To determine whether the difference in expression of rNa$_v$1.7 and rNa$_v$1.8 in the tsA201 mammalian cell line is associated with the presence or absence of trafficking signals in the C-terminus, we mutated the PY motif of Na$_v$1.8 and constructed Na$_v$1.8 chimeras containing the C-terminus of Na$_v$1.7. We showed that the proximal acid-rich region of the rNa$_v$1.7 C-terminus was able to restore high levels of rNa$_v$1.8 functional expression in the tsA201 mammalian cell line.

2. Materials and methods

2.1. Construction of recombinant rNa$_v$1.8 mutant and chimeric Na$^+$ channels

rNa$_v$1.8 C-terminus ubiquitin ProProSerTyr to Ala (PPSY→A, Tyr1923Ala) mutants were constructed using the following mutagenic sense and antisense primers: 5′-CG TCT TTC CCG CCA TCC GCT GAC AGT GTC ACC-3′ and 5′-GGT GAC ACT GTC AGC GGA TGG CGG GAA AGA CG-3′.

C-terminus rNa$_v$1.8 chimeras and double mutants were constructed using the following mutagenic sense and antisense primers. For the silent *Hpa*I site (Fig. 2): rNa$_v$1.7: 5′-C TTC CTG GTG GTG GTT ACC ATG TAC ATC GCT G-3′ and 5′-C AGC GAT GTA CAT GTT AAC CAC CAC CAG GAA G-3′; rNa$_v$1.8: 5′-C TTC CTC ATC GTG GTT AAC ATG TAC ATC GCA G-3′ and 5′-C TGC GAT GTA CAT GTT AAC CAC GAT GAG GAA G-3′. For the silent *Cla*I site (Fig. 2): rNa$_v$1.7: 5′-C GTC AAG AAT ATA TCA TCG ATA TAC ATA AAA GAT GG-3′ and 5′-CC ATA TTT TAT GTA TAT CGA TGA TAT ATT CTT GAC G-3′. For rNa$_v$1.8: 5′-CGC TCC TTG ACA CTA TCG ATC ACC CTG CAT GTG CC-3′ and 5′-GG CAC ATG CAG GGT GAT CGA TAG TGT CAA GGA GCG-3′. For the Gly1776Pro-Pro1781Ala double mutant: 5′-CC ACG CTC TCC CCC CCT CTT AGA ATC GCC AAA CCC AAC-3′ and 5′-GGT GGG TTT GGC GAT TCT AAG AGG GGG GGA GAG CGT GG-3′. For the Trp1848Arg-Leu1853Val double mutant 5′-CC ACC CTC CGG CGG AAG

*Corresponding author. Fax: (1)-418-656 4509.
E-mail address: mohamed.chahine@phc.ulaval.ca (M. Chahine).

Abbreviations: ER, endoplasmic reticulum; TTX, tetrodotoxin

0014-5793/04/$30.00 © 2004 Published by Elsevier B.V. on behalf of the Federation of European Biochemical Societies.
doi:10.1016/S0014-5793(04)00019-5

CAG GAA GAC GTC TCA GCC AC-3′ and 5′-GT GGC TGA GAC GTC TTC CTG CTT CCG CCG GAG GGT GG-3′.

Chimeras of $rNa_v1.8$ Na^+ channels in pCDNA3a containing the entire, proximal and distal carboxy-terminal segments of $rNa_v1.7$ Na^+ channels were constructed by introducing restriction enzyme sites as silent mutations by site-directed mutagenesis using the QuickChange™ site-directed mutagenesis kit according to the manufacturer's instructions (Stratagene, La Jolla, CA, USA).

The chimeras and the presence of the mutation were confirmed by automatic sequencing at the Laval University sequencing facility. The wild-type (WT) $rNa_v1.7$, $rNa_v1.8$ deletion mutant and the WT $hNa_v1.5$ in pcDNA1 constructs were purified using Qiagen columns (Qiagen, Chatsworth, CA, USA).

2.2. Transfection of tsA201 cell line

The tsA201 mammalian cell line was grown in high glucose Dulbecco's modified Eagle's medium supplemented with fetal bovine serum (10%), L-glutamine (2 mM), penicillin G (100 U/ml) and streptomycin (10 mg/ml) (Gibco BRL Life Technologies, Burlington, ON, Canada) and incubated in a 5% CO_2 humid atmosphere incubator. The tsA201 cells grown to 40–50% confluence on 100 mm plates were transfected with 5 μg of WT $rNa_v1.7$ and $rNa_v1.8$, mutant or chimeric $rNa_v1.8$ cDNAs. The β_1 subunit (5 μg) expressed by a bicistronic vector (pCD8-IRES-β_1) was co-transfected using the calcium phosphate method, which ensured that transfected cells that bound anti-CD8-a-coated beads (Dynabeads M-450 CD8-a) also expressed the β_1 subunit protein. Two to three days post transfection, the cells were incubated for 2 min in a medium containing anti-CD8-a-coated beads prepared according to the manufacturer's instructions (Dynal, Oslo, Norway). Unattached beads were removed by washing with extracellular solution. Cells expressing CD8-a on their surface fixed the beads and were distinguished from non-transfected cells by light microscopy.

2.3. Solutions and reagents

For whole-cell recordings, the patch pipette contained 35 mM NaCl, 105 mM CsF, 10 mM EGTA and 10 mM Cs-HEPES (pH 7.4). The bath solution contained 150 mM NaCl, 2 mM KCl, 1.5 mM $CaCl_2$, 1 mM $MgCl_2$, 10 mM glucose and 10 mM Na-HEPES (pH 7.4). The liquid junction potential between the patch pipette and the bath solution was corrected by −7 mV. Experiments were performed at room temperature (22–23°C).

2.4. Patch clamp method

Macroscopic sodium currents from transfected cells were recorded using the whole-cell configuration of the patch clamp technique [14]. Patch electrodes were made from 8161 Corning borosilicate glass and coated with Sylgard (Dow-Corning, Midland, MI, USA) to minimize their capacitance. Patch clamp recordings were performed using low resistance electrodes (<1 MΩ). A routine series resistance compensation using an Axopatch 200 amplifier (Axon Instruments, Foster City, CA, USA) was performed for values $>80\%$ to minimize voltage-clamp errors. The technical suitability of the voltage clamp control was addressed previously [15].

Voltage clamp command pulses were generated by a microcomputer using pCLAMP software v8.0 (Axon Instruments). Na^+ currents were filtered at 5 kHz, digitized at 10 kHz and stored on a microcomputer equipped with an AD converter (Digidata 1300, Axon Instruments). Experiments were performed 10 min after obtaining the whole-cell configuration to allow the current to stabilize and reduce the time-dependent shift of gating and to allow diffusion of the contents of the patch electrode. The reversal potential for each recording was calculated from the intercept of the linear interpolation of currents before and after reversal.

2.5. Statistical analysis

Where indicated, Student's *t*-tests were performed using SigmaPlot statistical software (Jandel Scientific Software, San Rafael, CA, USA). Differences were considered significant at $P<0.05$. Data are expressed using mean ± S.E.M.

3. Results

3.1. The effects of disrupting the $rNa_v1.8$ protein turnover motif

Families of inward Na^+ currents from tsA201 cells transfected with the parent channels $rNa_v1.7$ and $rNa_v1.8$ were evoked by a series of depolarizing pulses between −90 mV and +60 mV in 10 mV increments from a holding potential of −140 mV are shown in Fig. 1A,B, respectively. The tsA201 mammalian cell line transfected with $rNa_v1.7$ produced -1409 ± 156.5 pA/pF ($n=8$) levels of current. While a few cells transfected with $rNa_v1.8$ produced -15.6 ± 6.8 pA/pF ($n=7$) levels of current, most did not produce any current at all (Fig. 3). Endogenous TTX-S Na^+ currents in tsA201 cells were observed in some cells and were separated from the transfected $rNa_v1.8$ Na^+ currents by differences in peak voltages and kinetics. While endogenous TTX-S Na^+ currents peaked at more hyperpolarized potentials (−65 mV), $rNa_v1.8$ currents peaked at depolarized potentials of 0 mV.

To determine whether the low density of current levels of $rNa_v1.8$ in tsA201 was due to a rapid turnover of these channels at the plasma membrane, as observed with the cardiac $Na_v1.5$ Na^+ channel and Liddles ENaC mutant [10,11], we replaced tyrosine 1923 in the PY motif (ProProSerTyr, PPSY for $rNa_v1.7$ and $rNa_v1.8$ channels) by an alanine (Tyr1923-Ala: asterisk in Fig. 2). The tyrosine residue in the PPxY consensus site is crucial for the association with the WW domain of the Nedd4 ubiquitin ligase [16]. The whole-cell Na^+ currents of the PPSTyr1923Ala $rNa_v1.8$ mutant are shown in Fig. 1C. The mean peak current density of cells transfected with the PPSTyr1923Ala $rNa_v1.8$ mutant was -33.9 ± 5.8 pA/pF ($n=8$), which was statistically insignificant ($P>0.05$) compared to current levels of $rNa_v1.8$ expressed in the tsA201 cells (Fig. 3). This suggested that the low level of functional expression of the parent $rNa_v1.8$ was not due to rapid turnover at the cell membrane.

3.2. The effects of modifying the $rNa_v1.8$ C-terminal sequence

To gain a better understanding of the cause of the difference in current densities observed between $rNa_v1.7$ and $rNa_v1.8$ in tsA201 cells, the entire 233 amino acid $rNa_v1.8$ C-terminal region was replaced with the 226 amino acid $rNa_v1.7$ C-terminal segment. Since $rNa_v1.7$ channels are predominantly expressed in the large diameter fibers (L) and $rNa_v1.8$ channels are mainly found in the small diameter fibers (S), $rNa_v1.8$ chimeras containing the C-terminus of $rNa_v1.7$ are referred to as $S^{226aa}L$ (Fig. 2). A typical family of Na^+ currents from transfected cells expressing the chimera $S^{226aa}L$, evoked from a holding potential of −140 mV from −90 mV to +60 mV, is shown in Fig. 1D. The chimera $S^{226aa}L$ channels expressed a mean peak current of -50.6 ± 7.1 pA/pF ($n=18$, $P<0.05$) (Fig. 3). Other $rNa_v1.8$ chimera clones were constructed that contained either the first 155 amino acids ($S^{155aa}LS$) or the terminal 71 amino acids ($SS^{71aa}L$) of $rNa_v1.7$ (Fig. 2) in order to isolate the region responsible for the up-regulation of $rNa_v1.8$ in tsA201 cells. Interestingly, the $SS^{71aa}L$ chimera, which contains the section that shares the least homology between the two channels, did not rescue the expression of $rNa_v1.8$ (Fig. 3). The mean peak current densities of $SS^{71aa}L$ were similar to those observed with parent $rNa_v1.8$ channels (-30.5 ± 12.3 pA/pF, $n=8$). However, tsA201 cells transfected with the $S^{155aa}LS$ chimera expressed 4.8-fold more current. Average peak currents densities measured in tsA201 cells transfected with the $S^{155aa}LS$ chimera were -74.7 ± 6.8 pA/pF ($n=7$) versus the parent $rNa_v1.8$ channel, which expressed a peak current density of -15.6 ± 6.8 pA/pF ($n=7$) (Figs. 1E and 3).

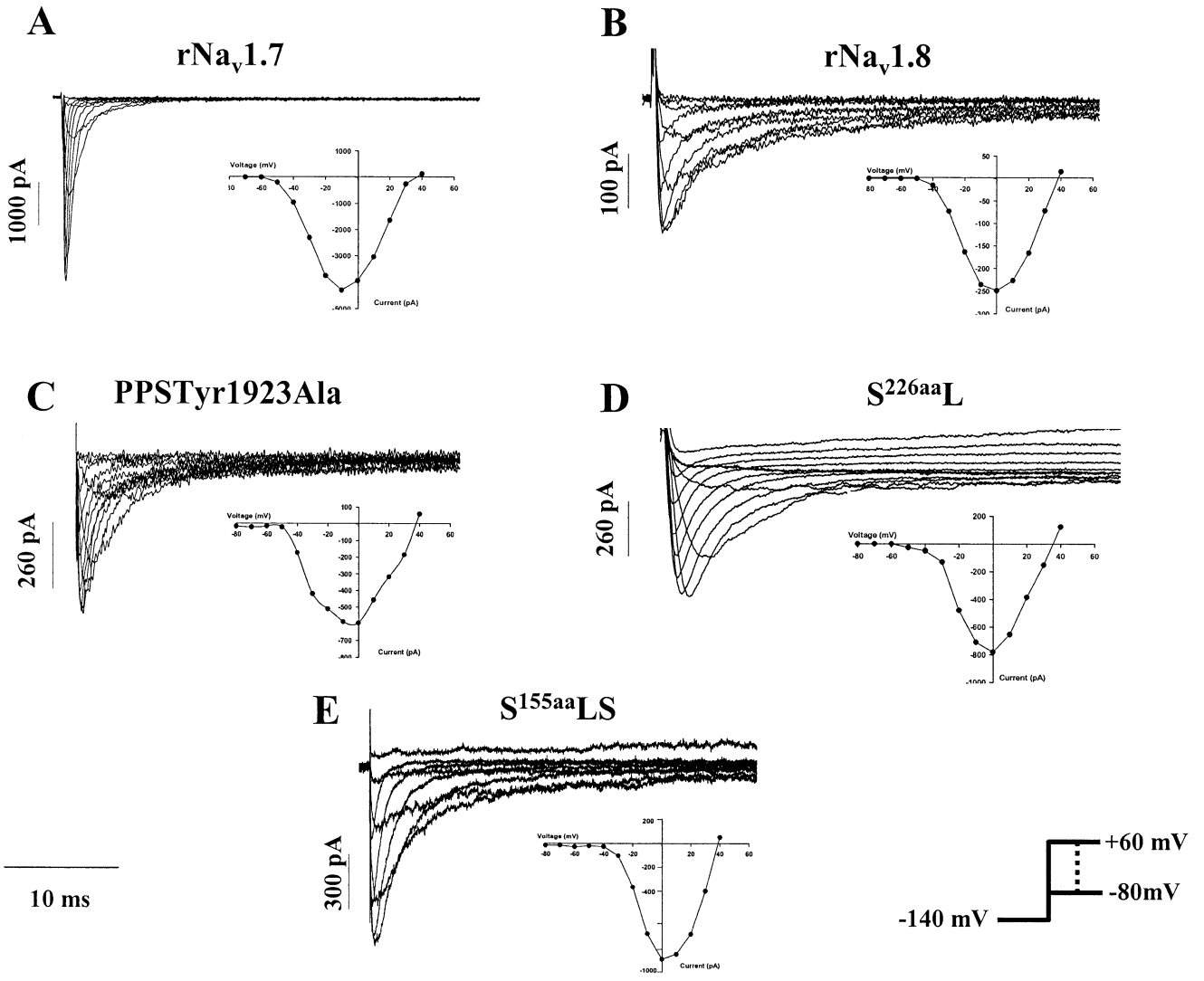

Fig. 1. Family of inward Na^+ currents. Currents were evoked between −90 mV and +60 mV at 10 mV intervals from a holding potential of −140 mV for parent rNa$_v$1.7 (A), parent rNa$_v$1.8 (B), ubiquitination mutant PPSTyr1923Ala (C) and chimeras created from the parent channels: S^{226aa}L (D) and S^{155aa}SL (E). S: rNa$_v$1.8 and L: rNa$_v$1.7. All the chimeras contained the four domains of rNa$_v$1.8. The S^{226aa}L chimera possessed the entire C-terminus of rNa$_v$1.7 (D) and S^{155aa}SL possessed the proximal 155 residues of the C-terminus of rNa$_v$1.7 (E). All parent channels, mutant channels and chimeras were co-expressed with the β_1 subunit.

3.3. The effects of voltage dependence and inactivation kinetics

To determine whether the increased peak current densities of rNa$_v$1.8 were due to changes in the biophysical properties of the channels, the voltage dependence of activation and inactivation and the time constant current decay of the parent channels, chimeras and point mutations were studied. The rNa$_v$1.8 C-terminal chimeras (S^{226aa}L and S^{155aa}LS) had a similar voltage dependence of activation as the parent rNa$_v$1.8 channels (Fig. 4A, Table 1). The slight shift in mid-points of steady-state inactivation observed for the S^{155aa}LS chimera was not statistically significant ($P = 0.046$). No shifts were also observed for the rNa$_v$1.8 channels with the ubiquitination site mutation (PPSTry1923Ala) (Fig. 3A, Table 1). Similarly, no shifts in steady-state inactivation were observed in any of the C-terminal rNa$_v$1.8 chimeras or mutants (Fig. 4B, Table 1). Furthermore, at a peak current voltage of 0 mV, no changes in the time constant of inactivation compared to the native rNa$_v$1.8 channels were observed (Table 1). The rNa$_v$1.7 channels had a significantly faster time constant of inactivation than the rNa$_v$1.8 channels, chimeras and point mutations and this was true over a range of voltages (−30 mV to +30 mV) (Fig. 4C).

4. Discussion

The goal of this study was to investigate the functional role of the C-terminal tail of two rat peripheral nerve voltage-gated Na^+ channels (rNa$_v$1.7 and rNa$_v$1.8) in a mammalian heterologous expression cell system (tsA201). In all the experiments, the tsA201 mammalian cell line was co-transfected with the channels and the auxiliary β_1 subunit since previous studies by our group had shown that β_1 causes a six-fold increase in peak current levels of Na$_v$1.8 in *Xenopus* oocytes [5,17]. We observed that rNa$_v$1.7 and rNa$_v$1.8 channels have differential expression levels in tsA201 (this study) and in CHO and COS (unpublished observation). The tsA201 cells transfected with parent rNa$_v$1.7 channels produced 90-fold higher mean peak current densities (−1409 ± 156.5 pA/pF)

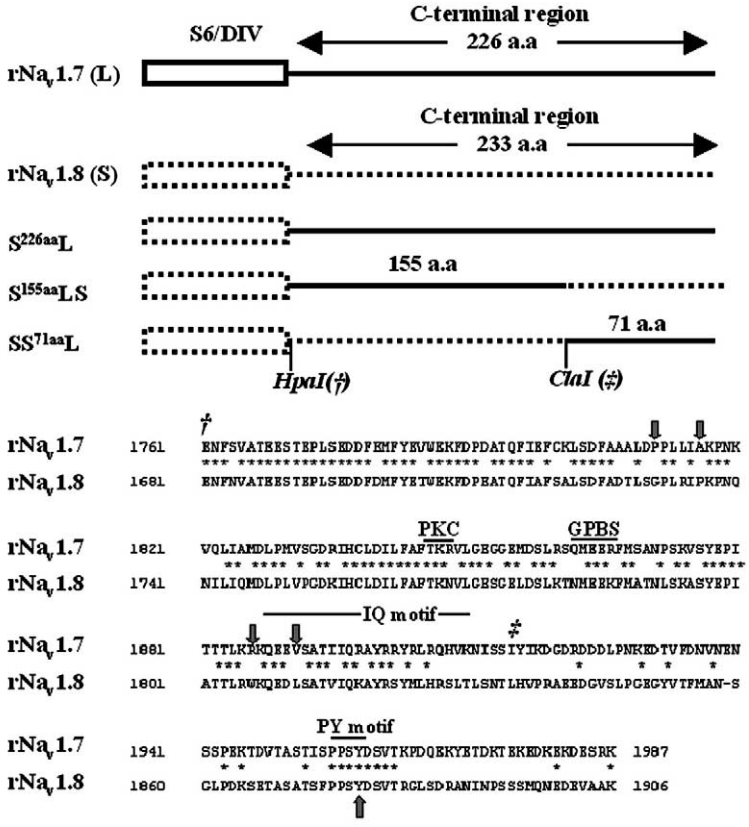

Fig. 2. Schema of the chimera construction and comparison of the amino acid sequences of $rNa_v1.7$ and $rNa_v1.8$ channels. A: Schematic representation of the construction of the $rNa_v1.8$ chimeras that contain the entire ($S^{226aa}L$) or a portion ($S^{155aa}SL$ and $SS^{71aa}L$) of the $rNa_v1.7$ C-terminus. B: Amino acid comparison of $rNa_v1.7$ and $rNa_v1.8$, where the putative PKC phosphorylation site (TRK/TRN), G protein binding site (GBPS, QMEEK/NMEEK), calmodulin binding site (IQ motif) and ubiquitin ligase binding site (PY motif) are highlighted. † and ‡ denote the *Hpa*I and *Cla*I restriction enzyme sites created by site-directed mutagenesis for the construction of the $rNa_v1.8$ C-terminal chimeras. Arrows indicate the positions of the double mutations on $rNa_v1.8$.

than cells transfected with $rNa_v1.8$, which had low expression levels (-15.6 ± 6.8 pA/pF).

Previous studies by Abriel et al. [10] on the expression of cardiac $Na_v1.5$ Na^+ channels in *Xenopus* oocytes showed that peak current expression is influenced by the internalization and degradation ubiquitin pathway [10]. They observed a three-fold increase in peak $rNa_v1.5$ Na^+ current levels when the PY motif, which is involved in promoting ubiquitination,

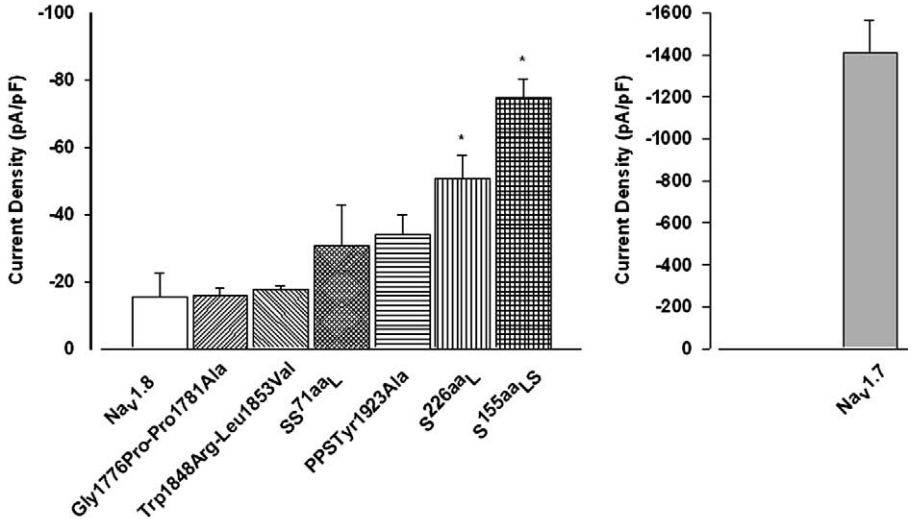

Fig. 3. Peak current densities of parent, mutant and chimera channels expressed in tsA201 cells in the presence of the β_1 subunit. A: Peak current densities (pA/pF) of the parent $rNa_v1.8$ channel and its mutants and chimeras. Only the $rNa_v1.8$ chimeric channels that possessed the entire or the proximal 155 amino acid residues of the $rNa_v1.7$ C-terminus expressed increased peak current densities. B: Peak current density of WT $rNa_v1.7$ channels. *Denotes levels of significance of $P < 0.05$.

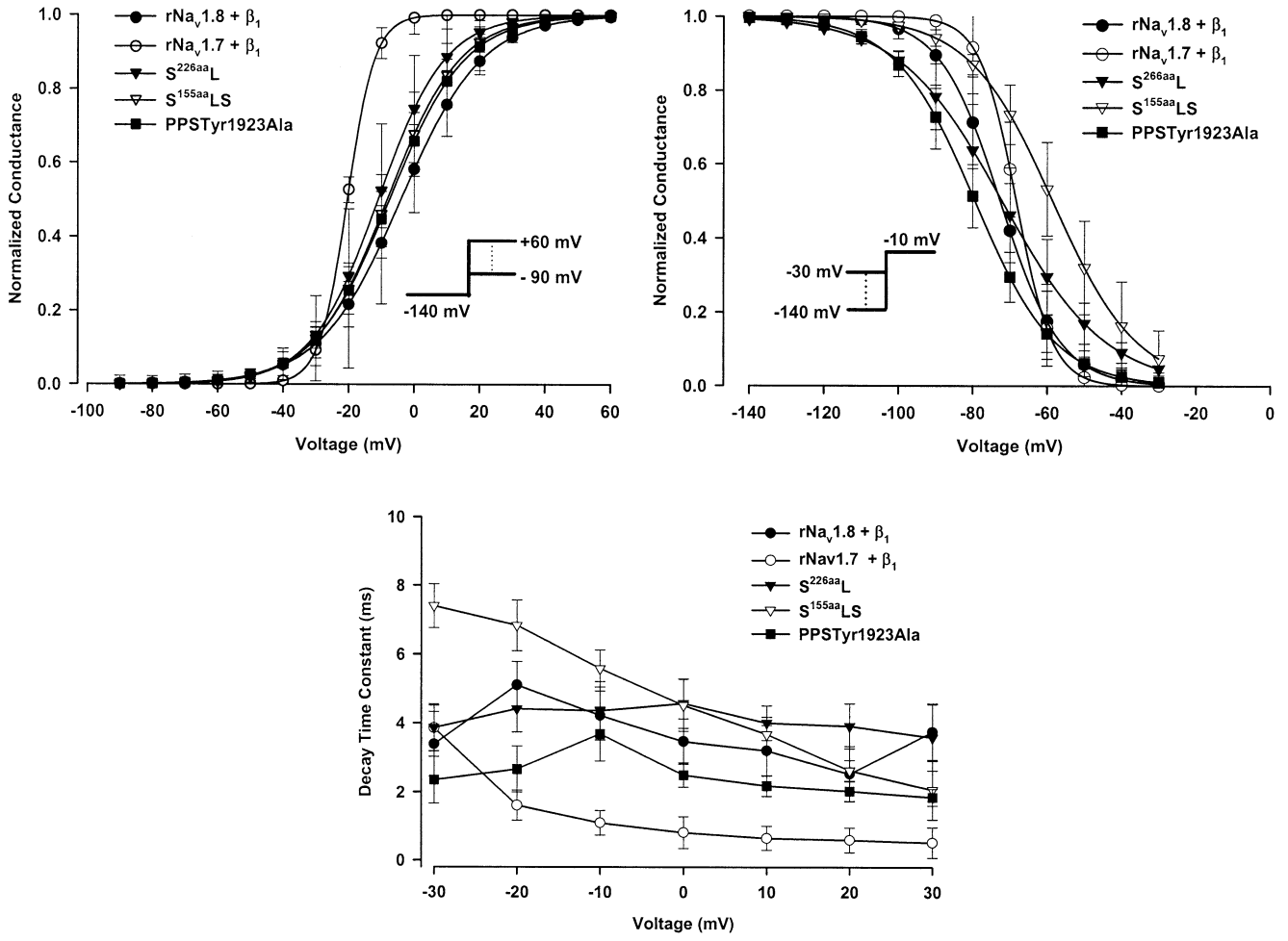

Fig. 4. Current–voltage relationship and voltage dependence of current decay of WT, mutant and chimera channels. A: The voltage dependence of steady-state activation (G_v) of rNa$_v$1.7, rNa$_v$1.8, mutant and rNa$_v$1.8 C-terminal chimeras was measured by applying a series of depolarizing pulses between −90 mV and +60 mV in 10 mV increments from a holding potential of −100 mV. The peak currents were measured and the relative conductance was calculated using the Boltzmann equation shown below. B: The voltage dependence of steady-state inactivation (h_∞) of rNa$_v$1.7, rNa$_v$1.8, mutant and rNa$_v$1.8 C-terminal chimeras was studied using a two-pulse protocol with a 500 ms conditioning pulse ranging from −140 mV to −30 mV and a standard pulse to 0 mV. The G_v and h_∞ smooth curves were fitted to a Boltzmann distribution: $I/I_{max} = 1/(1+\exp((V-V_{1/2})\ k_v))$, where $V_{1/2}$ and k_v are the voltage at which the channels are half-maximally activated and slope factor respectively. C: Voltage dependence of decay time constant of rNa$_v$1.7, rNa$_v$1.8, mutant and rNa$_v$1.8 C-terminal chimeras. The current decays of each peak current at different voltages were fitted with a single exponential (τ_h).

was disrupted. However, the disruption of the ubiquitination PY motif of rNa$_v$1.8 channels did not significantly improve the peak current densities of rNa$_v$1.8 in tsA201 cells. This suggests that the poor expression of rNa$_v$1.8 in the tsA201 cell line might not be due to a rapid turnover of the channels from the cell surface. rNa$_v$1.8 may, however, possess a yet to be identified ER export or retention signal.

Two classes of amino acid motifs have been proposed as export signals in K^+ channels: diacidic and dibasic [18]. Diacidic DXE-containing motifs are known to promote ER exiting of the rectifying potassium channel proteins Kir1.1, Kir2.1 and Kir4.1 [12,13]. On the other hand, dibasic sorting signals (K(X)KXX) are involved in the retention/retrieval of ER-resident proteins [19]. An amino acid comparison of the C-terminal segments of rNa$_v$1.7 and rNa$_v$1.8 showed that they share only 54% identity and that the rNa$_v$1.7 carboxy-terminus contains 13% more acidic residues. The mean peak current densities of rNa$_v$1.8 were significantly improved (3.2-fold, $P = 0.02$) when the entire 226 amino acid carboxy-terminal segment of rNa$_v$1.8 was replaced with that of rNa$_v$1.7 (S^{226aa}L). We also observed a similar increase in expression (four-fold) in oocytes injected (in the absence of the β$_1$ subunit) with the S^{226aa}L chimera compared to WT rNa$_v$1.8 channels (data not shown). The peak current densities of parent rNa$_v$1.8 channels were further increased 4.8-fold ($P = 0.01$) when the initial 155 amino acid segment (highly rich in acidic residues) of rNa$_v$1.8 was substituted for rNa$_v$1.7 (S^{155aa}LS).

Interestingly, no changes in the current decay time constant were observed in any of the chimeras, unlike what has been reported for other Na^+ channels [20,21]. The reason for this discrepancy is not known, but it could be channel-specific. Thus, for these two neuronal Na^+ channels, other regions of the protein may be important for modulating current decay. In addition, the increase in peak current densities was not associated with a change in either the voltage dependence of activation or inactivation. This suggests that the increase in peak current densities observed in the SL and S^{155aa}LS chimeras may be due to altered trafficking of the chimera rNa$_v$1.8

Table 1
Activation and inactivation parameters, time constant of decay currents and peak current densities of wild type and mutant channels and chimeras

Channel type	Voltage dependence of				τ_h (ms at 0 mV)	Peak current density (pA/pF)	n
	Activation (mV)		Inactivation (mV)				
	$V_{1/2}$	k_v	$V_{1/2}$	k_v			
$rNa_v1.7$	-20.4 ± 2.5	-4.2 ± 2.2	-68.3 ± 4.1	4.9 ± 1.1	0.8 ± 0.5	-1409 ± 12.2	8
$rNa_v1.8$	4.1 ± 1.2	-12.4 ± 2.9	-72.6 ± 3.1	8.1 ± 1.8	3.7 ± 1.3	-15.6 ± 6.8	7
PPSTry1923Ala	7.6 ± 3.2	-11.6 ± 0.9	-79.4 ± 3.9	10.78 ± 1.5	3.7 ± 0.7	-33.9 ± 5.8	9
$S^{226aa}L$	11.0 ± 3.7	-10.2 ± 0.3	-72.1 ± 5.7	13.9 ± 1.2	4.6 ± 2.0	-50.6 ± 7.2	18
$S^{155aa}SL$	8.3 ± 4.1	-11.1 ± 2.9	-58.5 ± 6.0	11.3 ± 0.8	4.5 ± 2.7	-74.7 ± 35.7	12

$V_{1/2}$ is the midpoint of the steady-state activation and inactivation, k_v is the slope factor of the steady-state activation and inactivation, τ_h is the time constant of current decay and n is the number of cells tested.

channels to the membrane surface. An amino acid comparison of the proximal 155 amino acid C-terminal region of $rNa_v1.8$ with $rNa_v1.7$ and other Na^+ channels ($rNa_v1.1$–1.3, $rNa_v1.4$ and $rNa_v1.5$) that are well expressed in tsA201) suggested that $rNa_v1.8$ possesses several amino acid differences. Two sets of closely situated amino acids (Gly1776–Pro1781 and Trp1848–Leu1853) were mutated to residues that corresponded to the $rNa_v1.7$ channel (Gly1776Pro–Pro1781Ala and Trp1848Arg–Leu1853Val respectively). Most tsA201 cells transfected with the Trp1848Arg–Leu1853Val double mutant had no currents while a few showed low levels of peak current densities (-17.49 ± 1.2 pA/pF, $n = 6$). Similar peak current densities were also observed with cells transfected with the Gly1776-Pro–Pro1781Ala double mutant (-15.9 ± 12.3 pA/pF, $n = 5$). This suggested that these residues in $rNa_v1.7$ are not involved in modulating peak current densities.

A database search of the 155 amino acid region did not identify any known potential transport signal motifs in this region of $rNa_v1.7$ or retention signal sequences in $rNa_v1.8$. Distinct ER processing signals may exist between the two channels, as has been observed between Kir2.1 and other Kir family members [12]. Since several mechanisms underlie the ER exit decision for an ion channel, including subunit composition (β subunits) [9], scaffolding and anchoring protein association [6–8] and the phosphorylation state [22,23], the export of $rNa_v1.8$ into tsA201 cells could co-depend on several of these factors. This also raises the possibility that the two channels may possess distinct ER export signals, which may provide a means of differential trafficking regulation when $rNa_v1.7$ and $rNa_v1.8$ are expressed in the same C-fiber neurons.

Acknowledgements: This study was supported by grants from the Heart and Stroke Foundation of Quebec (HSFQ) and the Canadian Institute of Health Research (CIHR) MOP-49502 awarded to M.C. M.C. is an Edwards Senior Investigator (Joseph C. Edwards Foundation). We would like to thank Dr. Ghayath Baroudi and Sylvie Pilote for their help in preparing the manuscript.

References

[1] Goldin, A.L. (2001) Annu. Rev. Physiol. 63, 871–894.
[2] Sangameswaran, L., Fish, L.M., Koch, B.D., Rabert, D.K., Delgado, S.G., Ilnicka, M., Jakeman, L.B., Novakovic, S., Wong, K., Sze, P., Tzoumaka, E., Stewart, G.R., Herman, R.C., Chan, H., Eglen, R.M. and Hunter, J.C. (1997) J. Biol. Chem. 272, 14805–14809.
[3] Sangameswaran, L., Delgado, S.G., Fish, L.M., Koch, B.D., Jakeman, L.B., Stewart, G.R., Sze, P., Hunter, J.C., Eglen, R.M. and Herman, R.C. (1996) J. Biol. Chem. 271, 5953–5956.
[4] Toledo-Aral, J.J., Moss, B.L., He, Z.J., Koszowski, A.G., Whisenand, T., Levinson, S.R., Wolf, J.J., Silos-Santiago, I., Halegoua, S. and Mandel, G. (1997) Proc. Natl. Acad. Sci. USA 94, 1527–1532.
[5] Vijayaragavan, K., O'Leary, M.E. and Chahine, M. (2001) J. Neurosci. 21, 7909–7918.
[6] Okuse, K., Malik-Hall, M., Baker, M.D., Poon, W.Y.L., Kong, H., Chao, M.V. and Wood, J.N. (2002) Nature 417, 653–656.
[7] Malik-Hall, M., Poon, W.Y.L., Baker, M.D., Wood, J.N. and Okuse, K. (2003) Mol. Brain Res. 110, 298–304.
[8] Liu, C., Dib-Hajj, S.D., Cummins, T.R. and Waxman, S.G. (2003) Soc. Neurosci. Poster 743.6.
[9] Shah, B.S., Stevens, E.B., Gonzalez, M.I., Bramwell, S., Pinnock, R.D., Lee, K. and Dixon, A.K. (2000) Eur. J. Neurosci. 12, 3985–3990.
[10] Abriel, H., Kamynina, E., Horisberger, J.D. and Staub, O. (2000) FEBS Lett. 466, 377–380.
[11] Abriel, H., Loffing, J., Rebhun, J.F., Pratt, J.H., Schild, L., Horisberger, J.D., Rotin, D. and Staub, O. (1999) J. Clin. Invest. 103, 667–673.
[12] Ma, D., Zerangue, N., Lin, Y.F., Collins, A., Yu, M., Jan, Y.N. and Jan, L.Y. (2001) Science 291, 316–319.
[13] Ma, D. and Jan, L.Y. (2002) Curr. Opin. Neurobiol. 12, 287–292.
[14] Hamill, O.P., Marty, A., Neher, E., Sakmann, B. and Sigworth, F.J. (1981) Pflügers Arch. 391, 85–100.
[15] Deschênes, I., Baroudi, G., Berthet, M., Barde, I., Chalvidan, T., Denjoy, I., Guicheney, P. and Chahine, M. (2000) Cardiovasc. Res. 46, 55–65.
[16] Einbond, A. and Sudol, M. (1996) FEBS Lett. 384, 1–8.
[17] Vijayaragavan, K., O'Leary, M.E. and Chahine, M. (2002) Biophys. J. 82, 25a.
[18] Aridor, M., Fish, K.N., Bannykh, S., Weissman, J., Roberts, T.H., Lippincott-Schwartz, J. and Balch, W.E. (2001) J. Cell Biol. 152, 213–229.
[19] Zerangue, N., Malan, M.J., Fried, S.R., Dazin, P.F., Jan, Y.N., Jan, L.Y. and Schwappach, B. (2001) Proc. Natl. Acad. Sci. USA 98, 2431–2436.
[20] Mantegazza, M., Yu, F.H., Catterall, W.A. and Scheuer, T. (2001) Proc. Natl. Acad. Sci. USA 98, 15348–15353.
[21] Deschênes, I., Trottier, E. and Chahine, M. (2001) J. Membr. Biol. 183, 103–114.
[22] Fitzgerald, E.M., Okuse, K., Wood, J.N., Dolphin, A.C. and Moss, S.J. (1999) J. Physiol. 516, 433–446.
[23] Zhou, J., Shin, H.G., Yi, J., Shen, W., Williams, C.P. and Murray, K.T. (2002) Circ. Res. 91, 540–546.